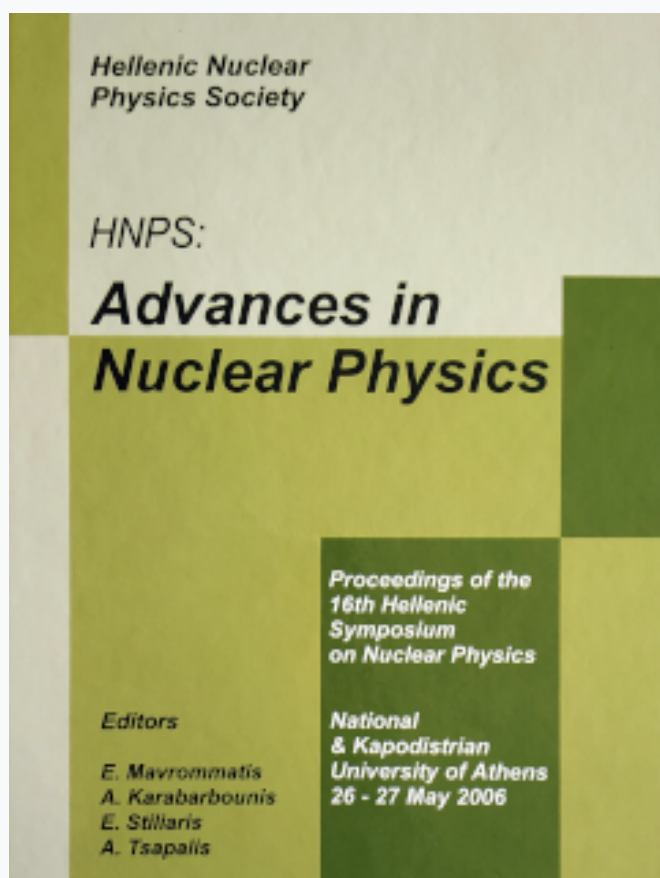


## HNPS Advances in Nuclear Physics

Vol 15 (2006)

HNPS2006



### Decay widths of Isoscalar Giant Monopole Resonances: regular and chaotic dynamics

P. K. Papachristou, E. Mavrommatis, V. Constantoudis, F. K. Diakonos, J. Wambach

doi: [10.12681/hnps.2622](https://doi.org/10.12681/hnps.2622)

#### To cite this article:

Papachristou, P. K., Mavrommatis, E., Constantoudis, V., Diakonos, F. K., & Wambach, J. (2020). Decay widths of Isoscalar Giant Monopole Resonances: regular and chaotic dynamics. *HNPS Advances in Nuclear Physics*, 15, 74–81. <https://doi.org/10.12681/hnps.2622>

Decay widths of Isoscalar Giant Monopole Resonances: regular and chaotic dynamics

P.K. Papachristou<sup>a\*</sup>, E. Mavrommatis<sup>a</sup>, V. Constantoudis<sup>b</sup>, F.K. Diakonos<sup>a</sup> and J. Wambach<sup>c</sup>

<sup>a</sup>Department of Physics, University of Athens, GR-15771, Athens, Greece

<sup>b</sup>Institute of Microelectronics (IMEL), NCSR "Demokritos", P.O. Box 60228

<sup>c</sup>Institut für Kernphysik, Technische Universität Darmstadt, Schlossgartenstr. 9, D-64289 Darmstadt, Germany

The decay of the Isoscalar Giant Monopole Resonances (IGMR) in the nuclei  $^{208}\text{Pb}$ ,  $^{144}\text{Sm}$ ,  $^{116}\text{Sn}$  and  $^{90}\text{Zr}$  is studied by means of a classical model consisting of several noninteracting nucleons moving in a potential well with an oscillating wall (nuclear surface). The motion of the nuclear surface is described by means of a collective variable which appears explicitly in the Hamiltonian as an additional degree of freedom. The total energy of the system is therefore conserved. Although the particles do not directly interact with each other, their motions are indirectly coupled by means of their interaction with the moving nuclear surface. Despite its simplicity and its purely classical nature, the model reproduces the trend of the experimental data which show that with increasing mass number the decay width decreases. Moreover, with the proper choice of the free parameters, the calculated decay widths are in good agreement with the experimental results. It seems that this agreement is dictated by the corresponding behaviour of the maximum Lyapunov exponent as a function of the system size.

## 1. INTRODUCTION

The decay of nuclear giant resonances [1,2] is a subject of intense theoretical (see for instance Refs.[3–7]) and experimental study [8–14]. It is known that in the dynamics of nuclear systems both chaotic behaviour and regular collective motion can occur. The interrelation between regular and chaotic motion as well as the role of chaoticity in the decay of nuclear excitations remain open problems. It is also known that both one body and  $n$ -body processes ( $n > 1$ ) contribute to the decay of nuclear excitations. By one-body processes we refer to the interaction of nucleons with the nuclear mean field or to the escape of nucleons into the continuum, and by  $n$ -body processes we refer to the interaction among nucleons. The relative contribution of one and  $n$ -body processes is still undetermined.

In the present work we focus mainly on one body processes using a model that can exhibit chaotic behaviour [3,5,15–17] and investigate the decay of the Isoscalar Giant Monopole Resonance (breathing mode) in several spherical nuclei. Our model is a simple classical Hamiltonian system which consists of particles moving in a Woods-Saxon well with an oscillating surface. This oscillation represents the Isoscalar Giant Monopole Resonance (IGMR) state in which the nuclear surface is oscillating radially, i.e. the spherical symmetry of the nucleus is preserved. The particles can interact with the surface and can exchange energy with it. The collective variable which describes the motion of the nuclear surface appears explicitly in the Hamiltonian of the

---

\*ppapachr@cc.uoa.gr

system as an additional degree of freedom, therefore the total energy of the system is conserved. Moreover, in our study we take into account the escape of nucleons from the oscillating well. The model we use can be thought of as a classical variation of the vibrating potential model [18].

We calculate the decay width of the IGMR in the spherical nuclei  $^{208}\text{Pb}$ ,  $^{144}\text{Sm}$ ,  $^{116}\text{Sn}$  and  $^{90}\text{Zr}$ , for which recent experimental data exist [13,12]. It is found that, under the appropriate assumptions, the trend of the experimental data can be reproduced, i.e. the decay width is a decreasing function of the mass number  $A$ . Moreover, with the proper choice of the free parameters, a good quantitative agreement with the experimental results can be obtained. With the same choice of the parameters the decay width of three other isotopes of  $\text{Sn}$  ( $^{112}\text{Sn}$ ,  $^{124}\text{Sn}$  and  $^{132}\text{Sn}$ ) is calculated. Finally, the fraction of the width due to escape is calculated for the above nuclei.

## 2. DESCRIPTION OF THE MODEL AND METHOD OF CALCULATION

Our system consists of  $N$  noninteracting nucleons of mass  $m$  moving in a Woods-Saxon well. The nucleons can exchange energy with the wall of the potential well (nuclear surface), which is considered to move in a harmonic oscillator potential with angular frequency  $\omega$  ([3,5,15–17]). A mass  $M$  is assigned to the nuclear surface and its motion around the equilibrium position  $R_0$  is described by the collective one-dimensional degree of freedom  $R$ . The Hamiltonian of the system equals

$$H = \sum_{i=1}^N \left[ \frac{p_{ri}^2}{2m} - \frac{V_0}{1 + \exp\left(\frac{r_i - R}{a}\right)} + \frac{L_i^2}{2mr_i^2} \right] + \frac{p_R^2}{2M} + \frac{1}{2}M\omega^2(R - R_0)^2 + \frac{L_R^2}{2mR^2}. \quad (1)$$

The angular momentum  $L_R$  of the collective degree of freedom  $R$  is taken equal to zero, i.e. the nuclear surface is not rotating. The angular momenta  $L_i$  of the particles are constants of the motion since the oscillating potential retains its spherical symmetry. The values of the parameters we use equal  $a = 0.67\text{fm}$ ,  $V_0 = 45\text{MeV}$  and  $R = 1.2A^{1/3}\text{fm}$ . The above values of  $a$  and  $V_0$  we use correspond to the nucleus  $^{208}\text{Pb}$ . For the angular frequency  $\omega$  we use the frequency of the IGMR obtained from the experimentally measured centroid energy  $E_x$ . The values of the frequency we use for the nuclei  $^{208}\text{Pb}$ ,  $^{144}\text{Sm}$ ,  $^{116}\text{Sn}$  and  $^{90}\text{Zr}$  equal  $13.96\text{MeV} \cdot \hbar^{-1}$ ,  $15.40\text{MeV} \cdot \hbar^{-1}$ ,  $15.85\text{MeV} \cdot \hbar^{-1}$  and  $17.81\text{MeV} \cdot \hbar^{-1}$  respectively (see Table 1)[13,12]. The parameters  $M/m$  and  $N$  will be considered as free parameters and their optimal values will be determined by comparing our results to the experimental data. More precisely, free parameters are the quantities  $M/m \cdot 100\%$  and  $N/A \cdot 100\%$  (see Eqs.4 and 5). With a simple rescaling of the equations of motion we find that the relevant parameters are  $N$ ,  $M/m$ ,  $R_0/a$  and  $V_0/(ma^2\omega^2)$ . Since the potential well is of finite depth, nucleons can escape from it yielding a contribution to the decay width.

For each nucleus we consider an ensemble of 5000 initial conditions selected according to the following prescription:

1. The energy  $E_R$  corresponding to the collective variable  $R$

$$E_R = \frac{p_R^2}{2M} + \frac{1}{2}M\omega^2(R - R_0)^2 \quad (2)$$

is taken equal to the experimentally measured centroid energy  $E_x$  of the IGMR. The corresponding initial momentum  $p_R$  is taken equal to zero.

2. The initial position  $r_i$  of the nucleon is selected from a uniform distribution in the interval  $[0, R]$ . The nucleon is a proton with a probability  $P = Z/A$  and a neutron with a probability  $1 - P$ .
3. The initial relative energy  $\Delta E_i$  of the nucleon with respect to the bottom of the potential well is selected using the density of energy states of a Fermi gas. The initial kinetic energy of the nucleon is therefore given by

$$T_i = -V_0 + \Delta E_i - \frac{V_0}{1 + \exp\left[\frac{r_i - R}{a}\right]}. \quad (3)$$

This energy is distributed between radial and angular motion by selecting the angle  $\theta_i$  randomly from a uniform distribution in the interval  $[0, \pi]$  ( $\theta_i$  is the angle between the vectors of the initial position and initial velocity) and by determining the radial component of the momentum and the angular momentum from the equations  $p_r = \sqrt{2mT} \cos \theta$  and  $L = \sqrt{2mTr} \sin \theta$  respectively.

In our study we neglect the Coulomb barrier. However, we have carried out calculations with the Coulomb barrier in the case of the nucleus  $^{208}\text{Pb}$  and our results for the decay width did not change appreciably. For each nucleus, we consider as free parameter the quantity

$$\Lambda = \frac{M}{mA} \cdot 100\%, \quad (4)$$

which is the percentage of the mass assigned to the collective degree of freedom and consequently can be thought of as a measure of the degree of collectivity of the motion. Apart from  $\Lambda$ , we also consider as a free parameter the quantity

$$\Xi = \frac{N}{A} \cdot 100\%, \quad (5)$$

which measures the percentage of nucleons that participate into the damping of the collective motion. For each nucleus and for a grid of values of  $\Xi$  and  $\Lambda$ , we calculate the mean value  $\langle R(t) \rangle$  of the collective variable  $R$  over the selected ensemble of 5000 orbits. We also calculate the mean value of the maximum Lyapunov exponent  $\langle \lambda_1 \rangle$  using the same initial conditions and integration time as the ones we used in the calculation of  $\langle R(t) \rangle$ . In order to estimate the decay width, we take the Fourier transform of  $\langle R(t) \rangle$  and calculate the standard deviation  $\sigma$  of the corresponding power spectrum in the frequency region around  $\omega$  where the power spectrum has a maximum. In order to obtain the width  $\Gamma$ , which corresponds to the full width at half maximum (FWHM) of an equivalent Gaussian fit to the power spectrum, we multiply  $\sigma$  by  $2\sqrt{\ln 4} \simeq 2.355$ .

### 3. RESULTS AND DISCUSSION

For the nuclei  $^{208}\text{Pb}$ ,  $^{144}\text{Sm}$ ,  $^{116}\text{Sn}$  and  $^{90}\text{Zr}$ , and for a  $9 \times 9$  grid of values for  $\Xi$  and  $\Lambda$ , we calculate the decay width  $\Gamma$  and the mean value of the largest Lyapunov exponent  $\langle \lambda_1 \rangle$ . Our results for  $\Gamma$  and  $\langle \lambda_1 \rangle$  are shown in Figs. 1 and 2 respectively. In Fig. 1, the lines in the  $\Xi$ - $\Lambda$  plane on which our results coincide with the experimental ones are also shown for the case of the nuclei  $^{208}\text{Pb}$ ,  $^{144}\text{Sm}$  and  $^{116}\text{Sn}$  (solid lines).

We first observe that the relationship between  $\langle \lambda_1 \rangle$  and  $\Gamma$  is in most cases what we would expect for a completely chaotic system. More specifically, for all values of  $\Xi$  and  $\Lambda$ , both  $\Gamma$  and  $\langle \lambda_1 \rangle$  decrease as  $A$  increases. Moreover, for each of the four nuclei studied, as  $\Xi$  and

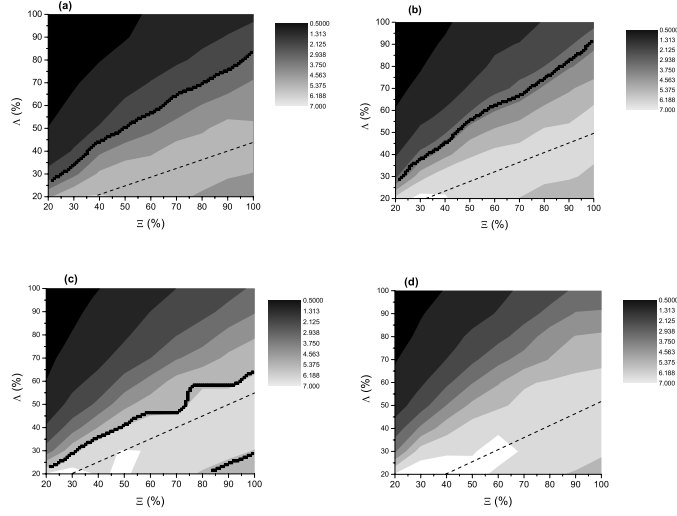


Figure 1. Decay width  $\Gamma$  of the IGMR as a function of the parameters  $\Xi$  and  $\Lambda$  for the nuclei (a)  $^{208}\text{Pb}$ , (b)  $^{144}\text{Sm}$ , (c)  $^{116}\text{Sn}$  and (d)  $^{90}\text{Zr}$ .

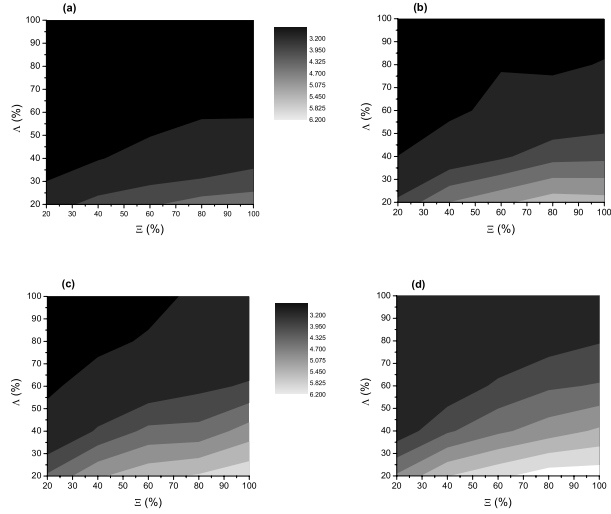


Figure 2. The mean value  $\langle \lambda_1 \rangle$  of the maximum Lyapunov exponent corresponding to the calculations of Fig.1 for the nuclei (a)  $^{208}\text{Pb}$ , (b)  $^{144}\text{Sm}$ , (c)  $^{116}\text{Sn}$  and (d)  $^{90}\text{Zr}$ .

Table 1

Experimental results for the excitation energy  $E_x$ , the decay width  $\Gamma_{exp}$  and the fraction  $\mu_{esc}$  of the width due to nucleon escape for the IGMR in the nuclei  $^{208}\text{Pb}$ ,  $^{144}\text{Sm}$ ,  $^{116}\text{Sn}$ ,  $^{90}\text{Zr}$ ,  $^{112}\text{Sn}$  and  $^{124}\text{Sn}$ .

Nucleus	$E_x(\text{MeV})$	$\Gamma_{exp}(\text{MeV})$	$\mu_{esc}$
$^{208}\text{Pb}$	$13.96 \pm 0.20$ [12]	$2.88 \pm 0.20$ [12]	$0.11 \pm 0.042$ [20]
$^{144}\text{Sm}$	$15.40 \pm 0.30$ [12]	$3.40 \pm 0.20$ [12]	-
$^{116}\text{Sn}$	$15.85 \pm 0.20$ [12]	$5.27 \pm 0.25$ [12]	-
$^{90}\text{Zr}$	$17.81 + 0.20, -0.32$ [13]	$7.86 + 0.89, -1.41$ [13]	$\simeq 0.08$ [19]
$^{112}\text{Sn}$	$15.67 \pm 0.11$ [14]	$5.18 + 0.40, -0.04$ [14]	-
$^{124}\text{Sn}$	$15.34 \pm 0.13$ [14]	$5.00 + 0.53, -0.03$ [14]	-

$\Lambda$  vary,  $\langle \lambda_1 \rangle$  and  $\Gamma$  vary with the same monotonicity except from a region with  $\Xi > 50\%$  and  $\Lambda < 30\%$ . Different monotonicities of  $\langle \lambda_1 \rangle$  and  $\Gamma$  have been reported in [16] and can be attributed to the existence of regular regions in phase space. In all cases, the decay width  $\Gamma$  seems to have its maximum value on a line with slope  $\approx 1/2$  on the  $\Xi - \Lambda$  plane (see Fig.1, dashed line).

Comparing our results for the decay width with the corresponding experimental ones, which are shown in Table 1, we observe that the trend of the experimental results is reproduced, i.e. the amplitude  $\Gamma$  decreases with increasing  $A$  for all values of  $\Xi$  and  $\Lambda$ . At a quantitative level, in the case of the nuclei  $^{208}\text{Pb}$  and  $^{144}\text{Sm}$ , our results coincide with the experimental ones on a curve which is close to a straight line (see Fig.1(a),(b)). The corresponding slopes determined by a least squares fit equal 0.69 and 0.75 respectively. Above (below) these lines, our results underestimate (overestimate) the experimental data. In the case of the nucleus  $^{116}\text{Sn}$ , our results coincide with the corresponding experimental on two lines with slopes 0.51 and 0.46 (see Fig.1(c)). For  $(\Xi, \Lambda)$  points between these lines our results overestimate the experimental whereas for points outside this region the experimental data are underestimated. In the case of the nucleus  $^{90}\text{Zr}$ , our results for  $\Gamma$  are smaller than the corresponding experimental ones for all values of  $\Xi$  and  $\Lambda$ . It seems that our model is more successful in the description of the decay width of medium-heavy nuclei. This may be due to the decreased collectivity of the IGMR in lighter nuclei ( $A < 100$ ) as well as to the increasing importance of two-body processes in these nuclei. In our model, as it has already been mentioned, although the particles do not interact with each other, their motions are indirectly coupled by means of their interaction with the moving nuclear surface and therefore part and not the whole effect of the two-body processes is taken into account.

In order to determine a region in the  $(\Xi, \Lambda)$  plane where there is an optimal agreement between our results and the corresponding experimental, we assume that all four nuclei can be described using the same values of  $\Xi$  and  $\Lambda$ , i.e. all the nuclei considered exhibit the same fraction of nucleons that take part in the damping and the same degree of collectivity. We calculate the sum  $\xi^2$  of the squares of the relative differences between our results and the experimental data

$$\xi^2 = \left( \frac{\Gamma_{Pb} - \Gamma_{Pb(exp)}}{\Gamma_{Pb(exp)}} \right)^2 + \left( \frac{\Gamma_{Sm} - \Gamma_{Sm(exp)}}{\Gamma_{Sm(exp)}} \right)^2 + \left( \frac{\Gamma_{Sn} - \Gamma_{Sn(exp)}}{\Gamma_{Sn(exp)}} \right)^2 + \left( \frac{\Gamma_{Zr} - \Gamma_{Zr(exp)}}{\Gamma_{Zr(exp)}} \right)^2, \quad (6)$$

as a function of the parameters  $\Xi$  and  $\Lambda$  ( $\text{Sn} \equiv ^{116}\text{Sn}$ ). The results are shown in Fig. 3. From this figure we observe that we have a good agreement with the experimental results in a region in the  $(\Xi, \Lambda)$  plane which is around a line with a slope approximately equal to 0.69. The optimal

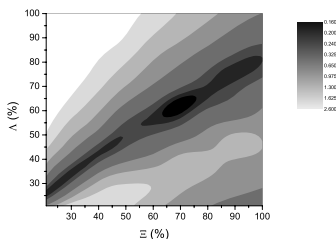


Figure 3. The sum  $\xi^2$  of the squares of the relative differences between our results and the experimental data for the nuclei  $^{208}\text{Pb}$ ,  $^{144}\text{Sm}$ ,  $^{116}\text{Sn}$  and  $^{90}\text{Zr}$  (see Eq.6).

agreement with the experimental results is obtained where  $\xi^2$  has its minimum value, i.e. for  $\Xi \simeq 69\%$  and  $\Lambda \simeq 62\%$ . We should note that by assuming a uniform sphere oscillating with linear radial displacement and velocity field, an oscillating mass  $M$  equal to  $3/5$  (0.6) of the total mass of the nucleus is deduced (scaling model,[21]). For the above mentioned values of  $\Xi$  and  $\Lambda$ , the calculated decay widths for the nuclei  $^{208}\text{Pb}$ ,  $^{144}\text{Sm}$ ,  $^{116}\text{Sn}$  and  $^{90}\text{Zr}$  equal 3.08MeV, 3.94MeV, 4.64MeV and 5.05MeV respectively. The above results along with the corresponding experimental ones are shown in Fig.4(a). From this figure, we observe that the discrepancy between our results and the experimental data increases as  $A$  decreases. This is possibly due to our assumption that all nuclei exhibit the same degree of collectivity, which should be modified when considering lighter nuclei. We should also mention the role of the two-body processes and the gradual change of the shape of the IGMR response which is observed for  $A \leq 100$  away from its symmetric single peaked Gaussian-like character. As for the dependence of  $\Gamma$  on  $A$  in our model, it is dictated by the classical mechanics of the system since the mean maximum Lyapunov exponent  $\langle \lambda_1 \rangle$  of the system has the same dependence on  $A$ , as can be seen from Fig.4(b).

For the above values of  $\Xi$  and  $\Lambda$  ( $\Xi = 69\%$  and  $\Lambda = 62\%$ ), we have also calculated the decay widths of the IGMR of two other Sn isotopes, namely  $^{112}\text{Sn}$  and  $^{124}\text{Sn}$ . Our calculation yields for the widths 4.68 MeV and 4.05 MeV respectively, whereas the experimentally obtained values equal 5.18 MeV and 5.00 MeV respectively[14]. In addition, for the same values of  $\Xi$  and  $\Lambda$ , we made a prediction for the decay width of the exotic nucleus  $^{132}\text{Sn}$  for which there is increased experimental interest. Our calculation yields  $\Gamma$  equal to 3.87 MeV. In our calculation, we have used as centroid energy  $E_x$  the value 15.29MeV, which is calculated theoretically in Ref.[22] by performing Hartree-Fock plus Random Phase Approximation calculations using the D1S parametrization of the Gogny two-body effective interaction.

We have also considered the fraction  $\mu_{esc}$  of the total decay width which is due to the escape of nucleons. It is defined as

$$\mu_{esc} = \frac{\Gamma - \Gamma'}{\Gamma}, \quad (7)$$

where  $\Gamma$  is the total decay width and  $\Gamma'$  is the decay width without taking into account the escape of particles. The latter is determined by excluding from our averaging the orbits with positive total energy. Our results are shown in Fig.5. From this figure, it can be seen that in the

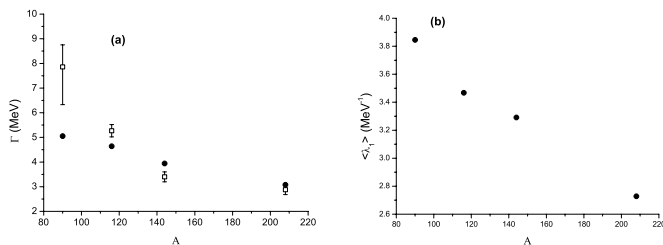


Figure 4. (a) The calculated values of the total decay width  $\Gamma$  for the nuclei  $^{208}\text{Pb}$ ,  $^{144}\text{Sm}$ ,  $^{116}\text{Sn}$  and  $^{90}\text{Zr}$  (circles) for the values of  $\Xi$  and  $\Lambda$  ( $\Xi \simeq 69\%$ ,  $\Lambda \simeq 62\%$ ) that minimize the quantity  $\xi^2$  (see Eq.6). The corresponding experimental results (squares) with their errors are also shown. (b) The corresponding values of the mean maximum Lyapunov exponent  $\langle \lambda_1 \rangle$ .

region of  $\Xi$  and  $\Lambda$  values in which agreement of our results for  $\Gamma$  with the experimental data is optimal,  $\mu_{esc}$  is between 0.20 and 0.28 for all nuclei under consideration. These values are larger than the corresponding experimental ones which are available only for the nuclei  $^{208}\text{Pb}$  and  $^{90}\text{Zr}$  (see Table 1). Inclusion of a Coulomb barrier leads to a decrease of  $\mu_{esc}$  by a fraction ranging from  $\approx 21\%$  (for  $^{90}\text{Zr}$ ) to  $\approx 35\%$  (for  $^{208}\text{Pb}$ ). However as our calculation is purely classical it does not account for the quantum tunneling of particles through the potential barrier. One should add that the experimental values for  $\mu_{esc}$  reported above refer to the direct escape width whereas our model probably includes part of the statistical decay width.

In conclusion, in this work we studied the decay of the Isoscalar Giant Monopole Resonance (IGMR) for several spherical nuclei using a classical model, in which a number of noninteracting nucleons move in an oscillating potential well and can exchange energy with the nuclear surface. The motion of the nuclear surface is described by a collective variable which appears explicitly in the Hamiltonian of the system as an additional degree of freedom. The total energy of the system is therefore conserved. Since there is no interaction between the particles, the model takes explicitly into account only one-body processes. Nevertheless, the particles interact indirectly with each other by means of the coupling of their motion to the motion of the oscillating nuclear surface. We find that our model, although of purely classical nature, can reproduce the trend of the experimental data which show that the decay width decreases with increasing mass number. Moreover, for medium-heavy nuclei, with the proper choice of the free parameters of the system, our results show a good agreement with the experimental data, at least comparable to the agreement of more sophisticated quantum models. The dependence of the decay width of the IGMR on the size of the nucleus has been found to be related to the characteristics of the underlying classical dynamics, i.e. to the maximum Lyapunov exponent.

## REFERENCES

1. J.P. Blaizot, Phys. Rep. 64 (1980) 171; G.F. Bertsch, P.F. Bortignon and R.A. Broglia, Rev. Mod. Phys. **55** (1983) 287 .
2. J. Speth and J. Wambach in *Electric and Magnetic Giant Resonances in Nuclei*, ed. J. Speth (World Scientific 1991), 1 ; ibid K.T. Knopfle and G.J. Wagner, 234.



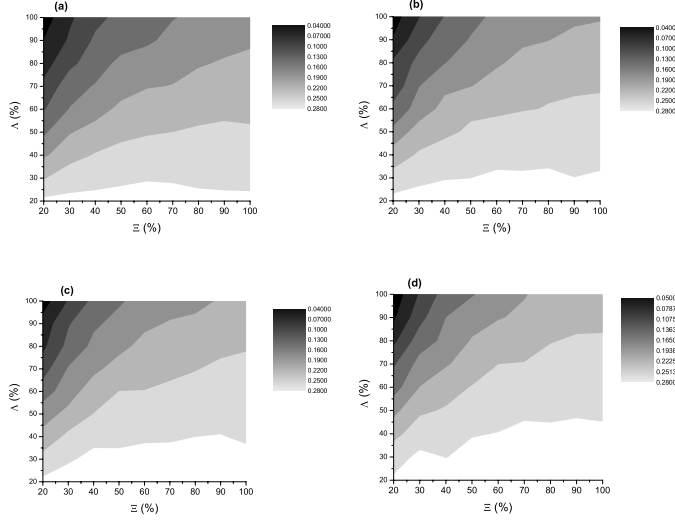


Figure 5. The fraction  $\mu_{esc}$  of the total decay width due to the escape of nucleons as a function of the parameters  $\Xi$  and  $\Lambda$  for the nuclei (a)  $^{208}\text{Pb}$ , (b)  $^{144}\text{Sm}$ , (c)  $^{116}\text{Sn}$  and (d)  $^{90}\text{Zr}$ .

3. G.F. Burgio, M. Baldo, A. Rapisarda and P. Schuck, Phys. Rev. C 52 (1995) 2475.
4. S. Drozdz, S. Nishizaki, J. Wambach and J. Speth, Phys. Rev. Lett. 74 (1995) 1075.
5. M. Baldo, G.F. Burgio, A. Rapisarda and P. Schuck, Phys. Rev. C 58 (1998) 2821.
6. D. Vretenar, N. Paar, P. Ring, G.A. Lalazissis, Phys. Rev. E 60 (1999) 308.
7. T. Papenbrock, Phys. Rev. C 61 (2000) 034602.
8. D. Youngblood, H.L. Clark and Y.-W. Lui, Phys. Rev. Lett. 82 (1999) 691.
9. Y.-W. Lui, H.L. Clark and D.H. Youngblood, Phys. Rev. C 61 (2000) 067307.
10. D.H. Youngblood et al, Phys. Rev. C 68 (2003) 057303.
11. M. Itoh et al, Phys. Rev. C 68 (2003) 064602.
12. D.H. Youngblood et al, Phys. Rev. C 69 (2004) 034315.
13. D.H. Youngblood et al, Phys. Rev. C 69 (2004) 054312.
14. Y.-W. Lui et al, Phys. Rev. C 70 (2004) 014307.
15. P.K. Papachristou, Ph.D. Thesis, University of Athens, Greece (2005).
16. P.K. Papachristou, E. Mavrommatis, V. Constantoudis, F.K. Diakonos and J. Wambach, Phys. Rev. E 73 (2006) 016204.
17. P.K. Papachristou, E. Mavrommatis, V. Constantoudis, F.K. Diakonos and J. Wambach, in submission.
18. P. Ring and P. Schuck, *The Nuclear Many Body Problem* (Springer-Verlag 1980).
19. M.L. Gorelik, S. Shlomo and M.H. Urin, Phys. Rev. C 62 (2000) 044301.
20. S. Brandenburg et al, Phys. Rev. C 39 (1989) 2448.
21. S. Stringari, Phys. Lett. B 108 (1982) 232.
22. S. Peru, W.F. Berger and P.F. Bortignon, Eur. Phys. J. A 26 (2005) 25.